Worsening urban ozone pollution in China from 2013 to 2017 – Part 2: The effects of emission changes and implications for multi-pollutant control

Yiming Liu[1], Tao Wang[1]

[1]Department of Civil and Environmental Engineering, The Hong Kong Polytechnic University, Hong Kong, 999077, China

Correspondence to: Tao Wang (cetwang@polyu.edu.hk)

Abstract. The Chinese government launched the Air Pollution Prevention and Control Action Plan in 2013, and various stringent measures have since been implemented, which have resulted in significant decreases in emissions and ambient concentrations of primary pollutants such as SO_2, NO_x, and particulate matter (PM). However, surface ozone (O_3) concentrations have still been increasing in urban areas across the country. In a previous analysis, we examined in detail the roles of meteorological variation during 2013–2017 in the summertime surface O_3 trend in various regions of China. In this study, we evaluated the effect of changes in multi-pollutant emissions from anthropogenic activities on O_3 levels during the same period, by using an up-to-date regional chemical transport model (WRF-CMAQ) driven by an interannual anthropogenic emission inventory. The CMAQ model was improved with regard to heterogeneous reactions of reactive gases on aerosol surfaces, which led to better model performance in reproducing the ambient concentrations of those gases. The model simulations showed that the maximum daily 8-hour average (MDA8) O_3 mixing ratio in urban areas increased by 0.46 ppbv per year (ppbv a^{-1}) ($p = 0.001$) from 2013 to 2017. In contrast, a slight decrease in MDA8 O_3 by 0.17 ppbv a^{-1} ($p = 0.005$) in rural areas was predicted, mainly attributable to the NO_x emission reduction. The effects of changes in individual pollutant emissions on O_3 were also simulated. The reduction of NO_x emission increased the O_3 levels in urban areas due to the non-linear NO_x-volatile organic compound (VOC) chemistry and decreasing aerosol effects; the slight increase in VOCs emissions enhanced the O_3 levels; the reduction of PM emissions increased the O_3 levels by enhancing the photolysis rates and reducing the loss of reactive gases on aerosol surfaces; and the reduction of SO_2 emissions resulted in a drastic decrease in sulfate concentrations, which increased O_3 through aerosol effects. In contrast to the unfavorable effect of the above changes in pollutant emissions on efforts to reduce surface O_3, the reduction of CO emissions did help to decrease the O_3 level in recent years. The dominant cause of increasing O_3 due to changes in anthropogenic emission varied geographically. In Beijing, NO_x and PM emission reductions were the two largest causes of the O_3 increase; in Shanghai, the reduction of NO_x and increase in VOC emissions were the two major causes; in Guangzhou, NO_x reduction was the primary cause; and in Chengdu, the PM and SO_2 emission decreases contributed most to the O_3 increase. Regarding the effects of decreasing concentrations of aerosols, the drop in heterogeneous uptake of reactive gases – mainly HO_2 and O_3 – was found to be more important than the increase in photolysis rates. The adverse effect of the reductions of NO_x, SO_2, and PM emissions on O_3 abatement in Beijing, Shanghai, Guangzhou, and Chengdu would have been avoided if the anthropogenic VOCs emission had been reduced by 24%, 23%, 20%, and 16%, respectively, from 2013 to 2017. Our analysis revealed that the NO_x reduction in recent years has helped to contain the total O_3 production in China. However, to reduce O_3 levels in major urban and industrial areas, VOCs emissions control should be added to the current NO_x-SO_2-PM policy.

1 Introduction

China has experienced severe haze pollution due to high concentrations of particulate matter (PM) in the past decade (e.g., Guo et al., 2014; Huang et al., 2014). To alleviate this air-quality problem, the Chinese government launched the Air Pollution Prevention and Control Action Plan in 2013 and has since implemented various emission control measures (Zhang et al., 2019). Anthropogenic emissions of sulfur dioxide (SO_2), nitrogen oxides (NO_x), carbon monoxide (CO), and $PM_{2.5}$ (PM with an aerodynamic diameter less than 2.5 μm) in China were reduced by 59%, 21%, 23%, and 33% from 2013 to 2017, respectively, while the emission of volatile organic compounds (VOCs) increased slightly (Zheng et al., 2018). As a result, ambient concentrations of SO_2, NO_2, CO, $PM_{2.5}$, and PM_{10} (PM with an aerodynamic diameter less than 10 μm) have declined, according to data from national environmental monitoring stations (http://www.mee.gov.cn; Fig. S1). However, surface ozone (O_3) concentrations in urban and surrounding areas increased from 2013 to 2017 (Lu et al., 2018). It is of critical importance to evaluate the effects of the existing control policies on atmospheric O_3 and refine these, if necessary, to improve overall air quality.

Ground-level O_3 is produced by chemical reactions involving NO_x, CO, and VOCs in the presence of sunlight. The key step in O_3 formation is the oxidation of nitric oxide (NO) by hydroperoxyl (HO_2) and alkylperoxyl (RO_2) to form NO_2, with subsequent photolysis of NO_2. It is well known that the relationship between the concentrations of O_3 and its precursors is non-linear and that NO_x can either suppress or increase O_3 formation depending on its abundance relative to VOCs (and CO) (e.g., Atkinson, 2000; Wang et al., 2017b). A large body of literature has established that O_3 formation in urban centers is generally VOCs-limited, that is, reducing VOCs emissions leads to a decrease in O_3 concentrations, but reducing NO_x emissions has the opposite result; in contrast, O_3 formation above rural areas is typically in the NO_x-limited or transitional regime, in which reducing NO_x emissions results in decreased O_3 (NRC, 1991; Atkinson, 2000; Wang et al., 2017b). Any process that perturbs HO_2 and RO_2 radicals will also affect O_3 production (e.g., Li et al., 2018a). Therefore, elucidating the chemical drivers of O_3 changes requires understanding the abundance and proportions of O_3 precursors and the radicals involved in O_3 formation. Aerosols in the atmosphere can affect O_3 concentrations via altering the solar actinic flux, which photolyzes gases to initiate oxidation (Li et al., 2011; Xing et al., 2017) and via heterogeneous reactions of reactive gases on aerosol surfaces (Li et al., 2018a; Stadtler et al., 2018; Lou et al., 2014).

Several studies have attempted to uncover the chemical drivers of the recent O_3 increase in China. Using a regional chemical transport model (WRF-CMAQ), Wang et al. (2019b) derived the variation of maximum daily 8-hour average (MDA8) O_3 due to emission changes during 2013–2015 by subtracting the simulated changes due to meteorological variations from the total observed changes. They found that the increase in O_3 concentrations in 2014–2015 relative to 2013 was mainly due to the emission changes, and speculated that the decrease in $PM_{2.5}$ concentrations and the reduction of NO_x emission in VOCs-limited regions could be the causes. In their study, however, the effects of emission changes during the study period were not explicitly simulated with interannual emissions. Li et al. (2019) utilized a global model (GEOS-Chem) to simulate the MDA8 O_3 in 2013 and 2017 and conducted sensitivity experiments for the effects of changes in $PM_{2.5}$ concentrations and anthropogenic emissions of O_3 precursors (NO_x and VOCs). Their results indicated that the drastic decrease in the $PM_{2.5}$ concentrations (~40%) during the period, which reduced the uptake of HO_2 on aerosol surfaces, was the main reason for the O_3 increase in the North China Plain (NCP). Wang et al. (2019a) simulated the effect of NO_x emission reduction during 2012–2016 with the WRF-CMAQ model in eastern China, which indicated increasing surface O_3 in urban areas due to the reduction of NO_x emissions. Yu et al. (2019) applied the Kolmogorov-Zurbenko filtering technique to the observed MDA8 O_3 during 2013–2017 in the Yangtze River Delta region, and concluded that the changes in O_3 precursor emissions contributed 76.7% to the O_3 increase, compared with 22% due to the decrease in $PM_{2.5}$ concentration.

We have been further investigating the meteorological and chemical driver(s) of the increasing summer surface O_3 in urban areas of China during 2013–2017 using an improved regional chemical transport model (WRF-CMAQ) driven by interannual meteorological data and anthropogenic emission inventories. The role of meteorological variation and total emission changes, the effect of changes in individual meteorological factors, and the impact of changes in long-range transport of O_3 and its precursors from outside the modeling domain, are discussed in a companion paper, Part 1 (Liu and Wang, 2020). The goal of the present work is to quantify (1) the effect of the changes in anthropogenic emissions of individual pollutants (NO_x, VOCs, CO, PM, SO_2, and NH_3) on urban O_3, which has not been addressed in the aforementioned studies but is important for further development of mitigation policy and (2) the effects of changes in aerosol concentrations on O_3 using a regional model with up-to-date radical sources and heterogeneous reactions. The improved model should give a more realistic account of gas-particle interactions crucial to O_3 formation, compared with its earlier version. In Section 2, we briefly introduce the model system and experiment setting; Section 3 first compares the simulated reactive gases that are subject to significant heterogeneous reactions with the observations reported in the literature. We then quantify the simulated trends of MDA8 O_3 in urban and rural areas during 2013–2017. We further investigate the response of MDA8 O_3 to the changes in individual pollutant emissions from anthropogenic activities from 2013 to 2017. We then examine the effect of aerosols on the O_3 changes by altering the photolysis rates and heterogeneous reactions. Lastly, we conduct numerical sensitivity experiments to calculate the magnitude of VOCs emission reductions needed to overcome the adverse effect of other pollutant reductions on the goal of O_3 mitigation. Section 4 gives the conclusions.

2 Methods

2.1 Model setting and emission inputs

The CMAQ model (version 5.2.1, the latest version) driven by the Weather Research and Forecasting (WRF) model and the interannual multi-resolution emission inventory for China (MEIC; http://www.meicmodel.org) was applied to conduct the simulations in this study. The model settings and emission inputs are described in the companion paper (Liu and Wang, 2020). The CMAQ model is an off-line chemical transport model (Byun and Schere, 2006) that does not consider the effect of pollutants on meteorology, but applies an in-line method (Binkowski et al., 2007) that uses the aerosol and O_3 concentrations predicted within a simulation to calculate the solar radiation and photolysis rates. As a result, the model takes into consideration the effect of aerosols on O_3 formation via altering the photolysis rates.

2.2 Updating heterogeneous reactions

The heterogeneous reactions in the original CMAQ model (version 5.2.1) include only the absorptions of NO_2, NO_3, and N_2O_5 on aerosol surfaces. To faithfully reproduce the effect of aerosols on O_3 via scavenging gaseous pollutants, we updated the heterogeneous reaction rate of NO_2 and NO_3 on the aerosol surface and incorporated additional heterogeneous reactions of gases into the CMAQ model, namely those of HO_2, O_3, OH, and H_2O_2 (refer to Table S2 in the companion paper (Liu and Wang, 2020) for the detailed heterogeneous reactions in the original and updated CMAQ models). The uptake coefficients (γ) of gases are the key parameters of heterogeneous reactions, but they vary according to factors such as aerosol water content and aerosol composition. In this study, we selected the "best guess" uptake coefficients for the gases, which have been widely used in chemical transport models in previous studies.

The uptake coefficient of N_2O_5 in the original CMAQ model was incorporated by Sarwar et al. (2012), based on the parameterization developed by Bertram and Thornton (2009) that considered its dependence on particle liquid water, particulate nitrate, and chloride.

The heterogeneous reaction rate of NO_2 in the original CMAQ model was suggested by Kurtenbach et al. (2001), based on the measurements at a relative humidity of 50% under dark conditions. Field and laboratory studies found that the rate not only depends on the relative humidity (Qin et al., 2009; Stutz et al., 2004) but also on sunlight intensity (Ndour et al., 2008; Stemmler et al., 2007). Fu et al. (2019) developed a new parameterization for the NO_2 heterogeneous reaction rate that considered both these factors, which has improved the simulation of the reaction product, nitrous acid (HONO). This parameterization was adopted in the updated CMAQ model.

Several laboratory studies have shown that the measured γ_{NO_3} ranges from 10^{-4} to 10^{-2} (Rudich et al., 1996; Exner et al., 1992; Moise et al., 2002). In the original CMAQ model, 10^{-4} was adopted as the value for γ_{NO_3} (Mao et al., 2013). A higher value (10^{-3}) was recommended by Jacob (2000) and was subsequently widely adopted in chemical transport models to investigate the effect of heterogeneous reactions on O_3 concentrations (Stadtler et al., 2018; Lou et al., 2014). This value was adopted in the updated CMAQ model.

The uptake coefficients of HO_2 vary widely, depending on the transition metal ions contained in aerosols (George et al., 2013; Huijnen et al., 2014). The heterogeneous reaction of HO_2 can produce either H_2O_2 or H_2O, depending on the particulate compounds in the aqueous phase. Li et al. (2019) conducted sensitivity experiments for the products of this reaction using the

GEOS-Chem model, finding little dependence on the reaction products when assessing the effect of aerosol on O_3 concentrations. Here, we let the heterogeneous reaction of HO_2 produce only H_2O_2, and adopt 0.2 for γ_{HO_2}, as recommended by Jacob (2000).

We used the value of 0.1 for the uptake coefficient of OH, based on the laboratory studies of DeMore et al. (1997). This value was also adopted by Zhang and Carmichael (1999) and Zhu et al. (2010) to explore heterogeneous reactions in a chemical transport model.

Previous laboratory and measurement studies of the heterogeneous reaction of O_3 have given a wide range of γ_{O_3}, from 10^{-6} to 10^{-4} on dust (Michel et al., 2002, 2003; Hanisch and Crowley, 2003), up to 10^{-4} on sodium chloride aerosol (Abbatt and Waschewsky, 1998), from 10^{-5} to10^{-3} on soot particles (Longfellow et al., 2000). Most previous modeling studies adopted $1x10^{-5}$ (Liao et al., 2004; Liao and Seinfeld, 2005; Pozzoli et al., 2008), while one recommended a lower value (3×10^{-6}) for dust particles (Bauer et al., 2004). We applied 10^{-5} to the uptake of O_3 on all the aerosols in our simulation.

DeMore et al. (1997) reported that the uptake coefficient of H_2O_2 on sulfuric acid and water surfaces ranged from 8×10^{-4} to 0.18. de Reus et al. (2005) found that using accommodation coefficients of 0.2 and 2×10^{-3} for HO_2 and H_2O_2, respectively, ensured agreement between simulated and observed values, under the assumption that H_2O_2 was produced in the heterogeneous reaction of HO_2. Thus, 2×10^{-3} was adopted for the uptake coefficient of H_2O_2 in this study.

The companion paper (Part 1; (Liu and Wang, 2020)) presented validation results of the updated CMAQ model against the observations of SO_2, NO_2, CO, O_3, and $PM_{2.5}$ from national environmental monitoring stations. In this study, we used the updated and original CMAQ models to simulate the concentrations of gases lost or produced on aerosol surfaces for the summer of 2013 and compared the simulated results with the observations reported in the literature (Table S1).

2.3 Experiment setting

We applied the updated WRF-CMAQ model to conduct simulations for the summer months (June, July, and August) from 2013 to 2017 with anthropogenic emissions. The shipping emissions were kept unchanged in the 5-year simulation, due to a lack of data for recent years. In Part 1 of our work (Liu and Wang, 2020), we showed the effect of changes in total anthropogenic emission on O_3 changes by comparing the O_3 levels in 2013 simulated using anthropogenic emissions from different years. In this study, three additional sets of modeling experiments were established. The first was designed to quantify the responses of O_3 to changes in individual pollutant emissions from 2013 to 2017, with the simulation in 2013 being regarded as the baseline experiment. The anthropogenic emissions of NO_x, VOCs, SO_2, CO, NH_3, PM (comprising PM_{10}, $PM_{2.5}$, and its components), black carbon (BC), organic carbon (OC), and combined NO_x/VOCs in 2013 were changed individually to those for 2017 in each sensitivity experiment (total number of experiments = 10), and the results were compared with those in the baseline experiment (Table S2). The second set of experiments was designed to investigate the effect of changes in aerosols on O_3 levels via altering the photolysis rates and heterogeneous reactions (Table S3). The individual effects of aerosol were deleted in each sensitivity experiment, and the results were compared with those in the baseline simulation. The corresponding differences showed the effects of aerosols on O_3 in 2013 in terms of photolysis rates or with respect to each heterogeneous reaction. A similar method was applied to the simulation of 2013 but with the 2017 anthropogenic emissions, and the difference was the effect of aerosols on the O_3 levels when the anthropogenic emissions of 2017 were applied in 2013. Finally, by comparing the results before and after the change of emissions from 2013 to 2017, the responses of O_3 to changes in aerosols via altering the photolysis rates and each heterogeneous reaction were quantified. Nineteen sensitivity experiments were performed. The third set of experiments was designed to calculate the magnitude that the VOCs emissions in 2017 would have had to be reduced by from 2013 to overcome the adverse effect of the changes in other pollutant emissions on O_3 reduction during this period. Based on the simulation of 2013 incorporating the 2017 anthropogenic emissions of all pollutants except VOCs, the VOCs emissions were reduced by 10%, 20%, 30% 40% and 50% in the sensitivity runs and the results were compared with those in the baseline experiment (Table S4). By comparing the response of the 2013 O_3 level to various VOCs emissions reductions, the required reduction of VOCs emissions was quantified.

3 Results

3.1 Comparison of the simulated and observed reactive gases

The simulated mixing ratios of reactive gases that are subject to significant heterogeneous reactions were compared with the observed values for the gases O_3, NO_2, NO_3, N_2O_5, HONO, $ClNO_2$, HO_2, OH, and H_2O_2 (Table S1). Except for O_3 and NO_2, which are measured by the regular national air monitoring network, the other gases were measured only in research-focused field campaigns. We compiled literature-reported summer concentrations of these gases for various years and compared these with the model-simulated values for 2013.

The uptake of NO_2 on wet aerosol surfaces can produce HONO in the atmosphere, which is an important source of OH radicals via photolysis. After the update of the CMAQ model, the predicted average NO_2 mixing ratio in China decreased from 19.2 ppbv to 16.6 ppbv, which came close to the observed value (15.1 ppbv). As a product of NO_2 uptake, the HONO mixing ratios increased significantly and approached the observed values in Beijing (Wang et al., 2017a) and Guangzhou (Qin et al., 2009; Li et al., 2012b). The decrease in NO_2 and increase in HONO were attributed to the increase in heterogeneous reaction rates of NO_2 due to the effects of relative humidity and sunlight intensity in the updated CMAQ model (Fu et al., 2019). Table S1 also presents the observed HONO mixing ratios at two coastal sites in Hong Kong (Li et al., 2018b; Xu et al., 2015), but their levels were substantially underpredicted because capturing such coastal characteristics is challenging for the model, due to its low horizontal resolution (36 km).

The simulated NO_3 mixing ratio decreased slightly (~1 pptv) due to the decrease in NO_2 and O_3 mixing ratios and the increase in γ_{NO_3} (from 10^{-4} to 10^{-3}). This decrease in NO_3 value was much smaller than the differences between the simulated and observed values in Shanghai (Wang et al., 2013) and Guangzhou (Li et al., 2012a). Nevertheless, the simulated NO_3 value moved closer to the observed value in Shanghai (Wang et al., 2013) after the heterogeneous reactions in the model were updated.

The parameterization of $\gamma_{N_2O_5}$ remains unchanged in the revised model. However, the decrease in NO_2 and O_3 levels resulted in a decrease in N_2O_5, and thus a decrease in $ClNO_2$. The simulated maximum N_2O_5 mixing ratio at the Wangdu site decreased by ~50% and thus agreed much better with the observed value (Tham et al., 2016). The simulated maximum $ClNO_2$ mixing ratio decreased slightly, by a margin much smaller than the biases between the simulation and observation. Table S1 presents the observed N_2O_5 and $ClNO_2$ values at a high-altitude site on Mount Tai (Wang et al., 2017c) and a coastal site in Hong Kong (Yan et al., 2019; Tham et al., 2014). Large differences between simulations and observations were found due to the complex terrains at these two sites, which are difficult for our model to simulate.

The CMAQ model predicted slightly lower the mixing ratios of HO_2 and OH radicals after the incorporation of their heterogeneous reactions. The changes were small, probably due to the scavenging effects of aerosols being counteracted by the increase in radical sources generated by HONO photolysis. The measured value for HO_2 contains an uncorrected contribution from RO_2 (Fuchs et al., 2011), which could explain in part the underestimation of HO_2 that occurred when using the updated and original models. For OH radicals, the mixing ratios simulated by both the original and updated models were comparable with the observed value in Wangdu (Tan et al., 2017), Beijing (Lu et al., 2013), and Guangzhou (Lu et al., 2012). The slight decrease in the OH mixing ratio after the update helped bring the simulation closer to the observations.

In the original CMAQ model, the MDA8 O_3 mixing ratio was overestimated by 11.4 ppbv. The bias was reduced to 6.8 ppbv with the updated heterogeneous reactions. In addition to the greater uptake of O_3 on aerosol surfaces, the updated model also includes other heterogeneous gas-aerosol reactions, weakening the atmospheric oxidation capacity and thus inhibiting O_3 formation.

The H_2O_2 mixing ratio decreased substantially from ~0.8 ppbv to ~0.2 ppbv, and the simulated value agreed well with the values recorded in Wangdu (Wang et al., 2016) and Beijing (Qin et al., 2018; Liang et al., 2013) after updating the model. Our results suggest that the chemical transport models are likely to substantially overestimate the H_2O_2 concentration if they do not include the sink of H_2O_2 on aerosol surfaces.

In summary, after updating the heterogeneous reactions in the CMAQ model, the simulations agreed better with the observations, especially for NO_2, HONO, O_3, and H_2O_2.

3.2 Variations in the urban and rural O_3

As most of the 493 air-quality monitoring sites established in 2013 are located in urban areas (refer to Fig. S1 in Part 1 (Liu and Wang, 2020)), the data from these stations mainly reflect the O_3 concentration changes in urban areas. The model simulations for the summer months from 2013 to 2017 over China give a comprehensive picture of the O_3 variations over the entire land areas of the country. Our previous analysis based on model simulations revealed that different trends in O_3 concentrations existed in urban and rural areas (Liu and Wang, 2020). In this study, we further quantified the O_3 trends in urban and rural areas over China using the nighttime light data from the Visible Infrared Imaging Radiometer Suite (VIIRS) Day/Night Band (DNB) (Fig. S2). We allocated the nighttime light data to the CMAQ modeling domain and averaged the values in each modeling grid cell. An urban area (rural area) was regarded as a grid-point with an averaged light-value ≥ (<) 2 nanowatts cm^{-2} sr^{-1}. Fig. S3 shows the spatial distribution of the urban and rural areas in China. The rates of changes in the MDA8 O_3 mixing ratios in urban and rural areas from 2013 to 2017 were then quantified based on the simulation results (Fig. 1). The model predicted that the MDA8 O_3 mixing ratio in urban areas increased at a rate of 0.46 ppbv per year (ppbv a^{-1}) ($p = 0.001$). This simulated increase (~2 ppbv from 2013 to 2017) in the nightlight-classified urban areas is much lower than the average increase observed at 493 sites in 74 cities (~9 ppbv, Fig. S1d). The discrepancy can be explained as follows. The urban areas determined using the nightlight data are not exactly the same as those 493 sites and cover some rural areas (with decreasing ozone) and additional small townships (Fig. S3). When we matched the modeled locations to the 493 observation sites, the model captured 57% of the rate of increase of MDA8 O_3 averaged at those sites (see Fig. S3 in Part 1 (Liu and Wang, 2020)). Part 1 also showed a large variability of meteorological impacts on O_3 in different regions (e.g., Beijing, Shanghai, Guangzhou, and Chengdu), and the simulated overall urban O_3 trend with a high confidence level ($p = 0.001$) suggests that this regional variability in meteorological impact can be 'averaged out', leading to a clearer urban O_3 trend driven by emission changes.

The simulated MDA8 O_3 mixing ratio in rural areas decreased at a rate of 0.17 ppbv a^{-1} ($p = 0.005$), which is supported by the recently reported rural ozone trends in China. Wang et al. (2019c) revealed no significant change in O_3 levels observed at a coastal site (Hok Tsui) in South China in the outflow of air mass from eastern China during 2007-2018. More recently, Xu et al. (2020) reported decreasing O_3 mixing ratios from 2013 to 2016 at two rural sites in BTH (Shangduanzi) and YRD (Linan). Overall, MDA8 O_3 mixing ratio in China exhibited a slightly decreasing trend (0.15 ppbv a^{-1}, $p = 0.006$) due to the decrease in a large rural area, which suggested that the ozone concentration has leveled off in recent years.

3.3 Response of O_3 to changes in multi-pollutant emissions

Fig. 2 presents the spatial distribution of changes in individual pollutant emissions in 2017 relative to 2013 (http://www.meicmodel.org). Significant reductions in anthropogenic emissions of NO_x, CO, SO_2, NH_3, PM_{10}, $PM_{2.5}$, BC, and OC were found in eastern China, while the emissions in western China decreased slightly, and even increased in some areas. NH_3 emission, which is primarily from agriculture (Fig. S4e), generally decreased across eastern China but increased in large areas in Neimenggu and northwestern China and some scattered areas in eastern China. VOCs emissions, which have not been subject to effective control measures, increased at scattered points (mostly industrial sites) over eastern China, except for Shandong province, where VOCs emissions decreased across the region. In summary, the emissions of NO_x, CO, SO_2, PM_{10},

$PM_{2.5}$, BC, and OC over mainland China were reduced by 21%, 24%, 61%, 38%, 33%, 29%, 34% in summer from 2013 to 2017, respectively (Fig. S4). In contrast, NH_3 emissions only decreased by 4%, and VOCs emissions increased by 5% during the same period.

Fig. 3 shows the spatial distribution of the effect of changes in these pollutant emissions on the MDA8 O_3 levels over China between 2013 and 2017. The average changes in O_3 mixing ratios in urban and rural areas (see Fig. S3 for their locations) are shown in Fig. 4a and 4b, respectively. The decrease in NO_x emissions caused an increase in O_3 mixing ratios in urban and industrial hot spots but a decrease in O_3 concentrations across a large swathe of rural areas (Fig. 3a). Quantitatively, the MDA8 O_3 mixing ratio increased by 0.30 ppbv in urban areas and decreased by 1.08 ppbv in rural areas, due to the NO_x emission reductions (Fig. 4a and b). In view of the small effects of changes in other pollutant emissions on rural O_3 mixing ratios (Fig. 4b), the decreasing trend of O_3 levels from 2013 to 2017 in rural areas was mainly ascribed to the reduction of NO_x emissions, consistent with the fact that O_3 formation in rural areas in China is generally limited by NO_x (e.g., Xing et al., 2011; Wang et al., 2017b). The increase in O_3 levels in urban areas due to NO_x reductions can be explained by two factors. First, most urban areas are in the VOCs-limited regime, where the reduction of NO_x emissions reduces the NO titration effect on O_3, resulting in increased O_3 concentrations. Second, the decrease in NO_x emissions can reduce the NO_3^- concentration and increase O_3 via weakening the aerosol effects.

In the simulation of VOCs emission changes, the spatial distribution of the O_3 levels closely tracked the changes in VOCs emissions (Fig. 3b). Specifically, the increase in VOCs emission caused an increase in the MDA8 O_3 mixing ratios across eastern China, except for Shandong province, where O_3 levels decreased due to the substantial reduction of VOCs emissions from the transportation sector according to the MEIC emission inventory (http://www.meicmodel.org). The simulation predicted an increase of 0.41 ppbv in the MDA8 O_3 mixing ratios from 2013 to 2017 due to the increase in VOCs emissions in urban areas (Fig. 4a). When changes in both the NO_x and VOCs emissions were simulated, it was the changes in NO_x emissions that primarily contributed to the changes in O_3 mixing ratio (Fig. 3c). In the simulation of changing CO emissions, the reduction of CO emissions reduced the O_3 level across China (Fig. 3d). A particularly large decrease in the O_3 mixing ratio was found in the NCP region, where both the CO emissions and their corresponding reduction were large. The CO emission reductions led to a decrease of 0.41 ppbv in MDA8 O_3 in urban areas (Fig. 4a). CO is an important O_3 precursor and plays a similar role to VOCs in O_3 formation, but the changes in its emission have rarely been discussed in previous studies of the causes of variations in O_3 concentrations. In fact, our results indicated that the reduction of CO emissions was the only government-implemented measure that reduced O_3 levels in recent years.

In addition to the effects of O_3 precursors, the emissions of other pollutants can also affect O_3 concentrations by altering photolysis rates and the loss of reactive gases from heterogeneous reactions. The reduction of SO_2 emissions increased the O_3 levels across China, particularly in northern China and the Sichuan Basin (SCB) (Fig. 3e). Quantitatively, SO_2 emissions reductions led to an increase of 0.75 ppbv in the MDA8 O_3 mixing ratios in urban areas (Fig. 4a), which was the largest cause of O_3 increases among all the pollutant emissions changes considered in this work. The SO_2 emission was reduced by more than 60% from 2013 to 2017, which resulted in a significant decrease in ambient SO_4^{2-} concentrations, and increased O_3 concentrations by increasing the photolysis rates and retarding the loss of reactive gases from heterogeneous reactions. The reduction of NH_3 emissions, an important precursor of ammonium, increased the O_3 mixing ratio across China in a similar way to the reduction in SO_2 emissions (Fig. 3f), but to a small extent, as the NH_3 emission was only reduced by 4%. Specifically, the increase in the MDA8 O_3 mixing ratios in urban areas due to the reduction of NH_3 emissions was only 0.06 ppbv (Fig. 4a), which was an insignificant fraction of the total increases in O_3 mixing ratios.

The reduction of primary PM emissions also enhanced O_3 formation across China, especially in the NCP and SCB regions (Fig. 3g). The MDA8 O_3 mixing ratios increased by 0.72 ppbv due to the PM emission reduction in urban areas (Fig. 4a). The effect of the changes in PM emissions on O_3 levels was comparable with that of the changes in SO_2 emissions, which indicated the significant O_3-promoting role played by reductions in both primary and secondary aerosols. BC and OC are among the components of direct aerosol emissions, and reductions in both were found to increase the O_3 levels (Fig. 3h and i). Although the reduction of BC emissions was smaller than the reduction in OC emissions, the increase in MDA8 O_3 due to the former was more significant. BC is an especially strong absorber of visible solar radiation in the atmosphere (Ramanathan and Carmichael, 2008), and therefore greatly retards photolysis rates by reducing the solar radiation reaching the earth's surface.

The dominant cause of O_3 increases due to emission changes varied among regions. Fig. 4 shows the average changes in O_3 mixing ratios due to changes in individual pollutant emissions in four megacities, Beijing, Shanghai, Guangzhou, and Chengdu (refer to Fig. S1 in part 1 for their locations), which are the representative cities in the Beijing-Tianjin-Hebei (BTH), Yangtze River Delta (YRD), Pearl River Delta (PRD), and SCB regions, respectively. In Beijing, NO_x and PM emission reductions were the two largest causes of rising O_3 levels, followed by SO_2 emission reductions. Air quality in the BTH region is a major concern, and strict emission-control measures have been implemented since 2013. As a result, the emissions of NO_x, $PM_{2.5}$, and SO_2 in BTH were reduced by 25%, 44%, and 65% from 2013 to 2017 (Fig. S5), respectively, which were generally larger reductions than occurred in other regions (Fig. 2). In Shanghai, the increase in the O_3 level was mainly due to the reduction of NO_x emissions and increase in VOCs emissions. This result is consistent with the finding of Yu et al. (2019) using the Kolmogorov-Zurbenko filtering technique, who also suggested that the changes in O_3 precursor emissions in the YRD contributed more to O_3 increases than did the decrease in $PM_{2.5}$ concentrations. In the YRD, NO_x emissions decreased by 19%, and that of VOCs increased by 10% from 2013 to 2017 (Fig. S6). Meanwhile, the $PM_{2.5}$ concentration in Shanghai was relatively low in summer. As a result, the effects of the PM and SO_2 emission reductions were smaller than those due to the changes in NO_x and VOCs emissions. In Guangzhou, the NO_x emission reduction was the dominant cause of the O_3 increase, while the effects of SO_2 and PM emission reductions on O_3 levels were insignificant. This result can likewise be ascribed to the low concentration of $PM_{2.5}$ in summer and relatively large reduction of NO_x emissions (Fig. S7) in the PRD. In Chengdu, the PM and SO_2 emission reductions contributed most to the increases in O_3 levels. The concentration of $PM_{2.5}$ in the SCB was high due to the basin topography and high emissions of both PM and its precursors. The significant reductions of $PM_{2.5}$ (35%) and SO_2 (65%) emissions in the SCB (Fig. S8) were thus the two major causes of the O_3 increase there. The inter-city variations in the dominant causes of increases in O_3 concentrations suggest that if the government wishes to alleviate urban O_3 pollution, they can adopt additional, localized emission-reduction measures as part of policies (see section 3.5).

3.4 The effects of aerosol on the O_3 variations

Aerosols in the atmosphere derived from direct emission and secondary formation can reduce photolysis rates and scavenge reactive gases from heterogeneous reactions, thereby inhibiting O_3 formation. Fig. 5 shows the spatial distribution of changes in the MDA8 O_3 mixing ratios due to the changes in the radiative and heterogeneous chemical effects of aerosols from 2013 to 2017 (see Methods). We isolated the effects of changes in seven heterogeneous reactions on the O_3 variations, and the average changes in O_3 levels in urban and rural areas are shown in Fig. 6a and 6b, respectively. As the $PM_{2.5}$ concentrations decreased substantially due to the reduction of anthropogenic pollutant emissions, the effects of aerosols on O_3 concentrations also decreased, which led to an increase in O_3 levels. The effects of the decrease in PM concentrations on O_3 were insignificant in western China. Significant increases in O_3 mixing ratios due to the decrease in various aerosol effects were found in urban and industrial areas of eastern China, particularly the NCP and SCB regions, where pollutant emissions were high and subject to a substantial reduction in the past few years. We found that the heterogeneous chemical effect, rather than the radiative effect, contributed most to the increase in O_3 levels driven by changes in PM concentrations. Quantitatively, the changes in photolysis rates and heterogeneous reactions increased the MDA8 O_3 mixing ratio by 0.30 ppbv and 2.12 ppbv in urban areas, respectively. In rural areas, the MDA8 O_3 mixing ratio increased by 0.87 ppbv via the heterogeneous chemical reactions on aerosols, while the effect of changes in photolysis rates was negligible. As for various heterogeneous reactions, the changes in individual reactions all increased MDA8 O_3 from 2013 to 2017. The decrease in the aerosol-sink effect of HO_2 contributed most to the O_3 increase due to changes in PM concentrations, followed by O_3, N_2O_5, and H_2O_2. The effects of changes in the heterogeneous reactions of NO_2, NO_3, and OH on the increase in O_3 levels were small.

The effect of the decrease in aerosol concentrations on O_3 levels varied by city. Significant effects were found in Beijing and Chengdu, where the $PM_{2.5}$ concentration was high and was subject to a large reduction by the implementation of emission-control measures. In contrast, the $PM_{2.5}$ concentration was lower in Shanghai and Guangzhou, and their O_3 levels were less affected by the decrease in aerosol concentrations.

Li et al. (2019) also investigated the effects of changes in photolysis rates and heterogeneous reactions on O_3 levels, using the GEOS-Chem model incorporating heterogeneous reactions of nitrogen oxides and HO_2. They quantified the effect of changes in photolysis rates by scaling the aerosol-extinction rate using the satellite-based aerosol optical depth changes, and the effect of changes in heterogeneous reactions by scaling the aerosol surface area using the measurement-based $PM_{2.5}$ changes from 2013 to 2017. They concluded that the increase in O_3 mixing ratios due to changes in PM concentrations could be largely ascribed to the decrease in the effect of HO_2 heterogeneous reaction. Using a regional model and adopting different experimental settings, our work uncovered a similar and substantial effect of HO_2 uptake on increases in O_3 levels due to changes in PM concentrations. In addition, with more heterogeneous reactions implemented in the CMAQ model, we found that the uptake of O_3 on aerosol surfaces was also important, following HO_2.

3.5 The anthropogenic VOCs emission control to reduce O_3

The results in the preceding sections show that although the CO emission reductions contributed to a decrease in O_3 levels, the reductions of SO_2, NO_x, and PM emissions had a counterproductive effect on O_3 reductions, resulting in a substantial increase in urban O_3 concentrations due to the non-linear NO_x-VOCs chemistry and the weakening of aerosol effects. To alleviate these negative effects of PM-targeted control policies and thereby reduce ambient O_3 concentrations, we found that anthropogenic VOCs emissions must also be reduced, alongside reductions in emissions of other pollutants.

Fig. 7 presents the changes in the MDA8 O_3 mixing ratios from its 2013 value, where the 2013 VOCs emissions were decreased from 0% to 50% while the 2017 emissions of other pollutants were retained (see Methods). The MDA8 O_3 mixing ratios in the four studied megacities decrease linearly with the reduction of VOCs emissions, reflecting that O_3 formation in these cities is VOCs-limited. Compared with the O_3 level in 2013, the VOCs emissions would have needed to be reduced by approximately 20% to prevent increases in MDA8 O_3 from 2013 to 2017. This suggests that the adverse effects of the reductions of NO_x, SO_2, and PM emissions on urban O_3 could have been avoided with a ~20% reduction of VOCs emissions from 2013 to 2017. The exact reductions of VOCs emissions required vary among the four megacities: Beijing (24%), Shanghai (23%), Guangzhou (20%), and Chengdu (16%). In Beijing (BTH region), the drastic reductions of NO_x, SO_2, and PM emissions would have necessitated a more substantial reduction of VOCs emissions to counteract the O_3 increase. In Shanghai (YRD region) and Guangzhou (PRD region), the increase in O_3 concentrations due to the reductions in NO_x emissions also calls for a significant reduction in VOCs emissions. In Chengdu (SCB region), a smaller VOCs emission reduction is needed because of the relatively small increase in O_3 concentrations due to changes in other emissions. We also found that the required percentage reductions of VOCs emissions in each city were comparable with the actual percentage reductions in NO_x emissions (25%, 19%, 18%, and 14% for Beijing, Shanghai, Guangzhou, and Chengdu, respectively), suggesting that similar percentage reductions of VOCs and NO_x would have prevented the increase in O_3 levels from 2013 to 2017.

Our results have important implications for air-pollution control policy in the coming years. In 2018, the Chinese government issued a Three-Year Action Plan (2018–2020) mandating further reductions of national SO_2 and NO_x emissions by at least 15% by the year 2020 compared with those in the year 2015, and an 18% reduction in ambient $PM_{2.5}$ concentrations in cities currently not compliant with China's $PM_{2.5}$ standards (http://www.gov.cn/zhengce/content/2018-07/03/content_5303158.htm). This implies that if VOCs emissions are not reduced in the near future, the O_3 pollution in major cities will continue to worsen. Therefore, we suggest VOCs emission controls be implemented together with the PM-targeted measures in order to alleviate the urban O_3 pollution.

4 Conclusions

This study has quantified the effects of changes in pollutant emissions from anthropogenic activities on the summer surface O_3 concentrations over China from 2013 to 2017. The control measures, while successful in reducing the concentrations of primary pollutants and particulate matter, were found to increase urban O_3 but reduce rural O_3; overall, the NO_x emission reduction has helped to contain total ozone production in China. The reduction in NO_x emission and slight increase in VOC emissions led to ozone increase in urban areas due to the non-linear chemistry of O_3, and the large reductions in PM and SO_2 emissions contributed to urban ozone increase resulting from the complex effects of aerosols on radiation and chemical reactions. Among the primary PM components, the emission decrease in BC increased O_3 more than that for OC despite its smaller reduction compared to OC, resulting from BC being a strong absorber of solar radiation. The dominant causes of the urban ozone increase due to emission change varied among different cities, and they were NO_x and PM in Beijing, NO_x and VOC in Shanghai, NO_x in Guangzhou, and PM and SO_2 in Chengdu. For the aerosol effects, the decrease in heterogeneous uptake of reactive gases was more important than the increase in photolysis rates. Only the CO emission cut helped to decrease urban ozone. Our results show that comparable percentage reductions in anthropogenic VOCs to that achieved for NO_x could have prevented the increases in urban O_3 concentrations. We thus recommend that VOCs control be implemented in current and future emission-reduction measures to improve the overall air quality. In view of the importance and complexity of the uptake of reactive gases on aerosol surfaces, more research should be conducted in this area.

Author contributions

T.W. initiated the research. Y.M.L. and T.W. designed the research framework. Y.M.L. modified the model and performed model simulations. T.W. and Y.M.L. analyzed the results and wrote the paper.

Competing interests

The authors declare that they have no conflict of interest.

Code/Data availability

The code or data used in this study are available upon request from Yiming Liu (yming.liu@polyu.edu.hk) and Tao Wang (cetwang@polyu.edu.hk).

Acknowledgments

This work was supported by the Hong Kong Research Grants Council (T24-504/17-N) and the National Natural Science Foundation of China (91844301). We would like to thank Prof. Qiang Zhang from Tsinghua University for providing the emission inventory, and Dr. Xiao Fu from The Hong Kong Polytechnic University for sharing the model codes of HONO sources.

References

Abbatt, J. P. D., and Waschewsky, G. C. G.: Heterogeneous Interactions of HOBr, HNO3, O3, and NO2 with Deliquescent NaCl Aerosols at Room Temperature, The Journal of Physical Chemistry A, 102, 3719-3725, 10.1021/jp980932d, 1998.

Atkinson, R.: Atmospheric chemistry of VOCs and NOx, Atmos. Environ., 34, 2063-2101, Doi 10.1016/S1352-2310(99)00460-4, 2000.

Bauer, S. E., Balkanski, Y., Schulz, M., Hauglustaine, D. A., and Dentener, F.: Global modeling of heterogeneous chemistry on mineral aerosol surfaces: Influence on tropospheric ozone chemistry and comparison to observations, J Geophys Res-Atmos, 109, 10.1029/2003jd003868, 2004.

Bertram, T. H., and Thornton, J. A.: Toward a general parameterization of N2O5 reactivity on aqueous particles: the competing effects of particle liquid water, nitrate and chloride, Atmos Chem Phys, 9, 8351-8363, DOI 10.5194/acp-9-8351-2009, 2009.

Binkowski, F. S., Arunachalam, S., Adelman, Z., and Pinto, J. P.: Examining Photolysis Rates with a Prototype Online Photolysis Module in CMAQ, 46, 1252-1256, 10.1175/jam2531.1, 2007.

Byun, D., and Schere, K. L.: Review of the governing equations, computational algorithms, and other components of the models-3 Community Multiscale Air Quality (CMAQ) modeling system, Appl Mech Rev, 59, 51-77, 10.1115/1.2128636, 2006.

de Reus, M., Fischer, H., Sander, R., Gros, V., Kormann, R., Salisbury, G., Van Dingenen, R., Williams, J., Zöllner, M., and Lelieveld, J.: Observations and model calculations of trace gas scavenging in a dense Saharan dust plume during MINATROC, Atmos. Chem. Phys., 5, 1787-1803, 10.5194/acp-5-1787-2005, 2005.

DeMore, W. B., Sander, S. P., Golden, D. M., Hampson, R. F., Kurylo, M. J., Howard, C. J., Ravishankara, A. R., Kolb, C. E., and Molina, M. J.: Chemical kinetics and photochemical data for use in stratospheric modeling, National Aeronautics and Space Administration and Jet Propulsion Laboratory, California Institute of Technology, California, 1997.

Exner, M., Herrmann, H., and Zellner, R.: Laser-Based Studies of Reactions of the Nitrate Radical in Aqueous Solution, 96, 470-477, 10.1002/bbpc.19920960347, 1992.

Fu, X., Wang, T., Zhang, L., Li, Q., Wang, Z., Xia, M., Yun, H., Wang, W., Yu, C., Yue, D., Zhou, Y., Zheng, J., and Han, R.:

The significant contribution of HONO to secondary pollutants during a severe winter pollution event in southern China, Atmos. Chem. Phys., 19, 1-14, 10.5194/acp-19-1-2019, 2019.

Fuchs, H., Bohn, B., Hofzumahaus, A., Holland, F., Lu, K. D., Nehr, S., Rohrer, F., and Wahner, A.: Detection of HO₂ by laser-induced fluorescence: calibration and interferences from RO₂ radicals, Atmos. Meas. Tech., 4, 1209-1225, 10.5194/amt-4-1209-2011, 2011.

George, I. J., Matthews, P. S. J., Whalley, L. K., Brooks, B., Goddard, A., Baeza-Romero, M. T., and Heard, D. E.: Measurements of uptake coefficients for heterogeneous loss of HO2 onto submicron inorganic salt aerosols, Phys Chem Chem Phys, 15, 12829-12845, 10.1039/c3cp51831k, 2013.

Guo, S., Hu, M., Zamora, M. L., Peng, J. F., Shang, D. J., Zheng, J., Du, Z. F., Wu, Z., Shao, M., Zeng, L. M., Molina, M. J., and Zhang, R. Y.: Elucidating severe urban haze formation in China, P Natl Acad Sci USA, 111, 17373-17378, 10.1073/pnas.1419604111, 2014.

Hanisch, F., and Crowley, J. N.: Ozone decomposition on Saharan dust: an experimental investigation, Atmos. Chem. Phys., 3, 119-130, 10.5194/acp-3-119-2003, 2003.

Huang, R. J., Zhang, Y. L., Bozzetti, C., Ho, K. F., Cao, J. J., Han, Y. M., Daellenbach, K. R., Slowik, J. G., Platt, S. M., Canonaco, F., Zotter, P., Wolf, R., Pieber, S. M., Bruns, E. A., Crippa, M., Ciarelli, G., Piazzalunga, A., Schwikowski, M., Abbaszade, G., Schnelle-Kreis, J., Zimmermann, R., An, Z. S., Szidat, S., Baltensperger, U., El Haddad, I., and Prevot, A. S. H.: High secondary aerosol contribution to particulate pollution during haze events in China, Nature, 514, 218-222, 10.1038/nature13774, 2014.

Huijnen, V., Williams, J. E., and Flemming, J.: Modeling global impacts of heterogeneous loss of HO₂ on cloud droplets, ice particles and aerosols, Atmos. Chem. Phys. Discuss., 2014, 8575-8632, 10.5194/acpd-14-8575-2014, 2014.

Jacob, D. J.: Heterogeneous chemistry and tropospheric ozone, Atmos. Environ., 34, 2131-2159, 2000.

Kurtenbach, R., Becker, K. H., Gomes, J. A. G., Kleffmann, J., Lorzer, J. C., Spittler, M., Wiesen, P., Ackermann, R., Geyer, A., and Platt, U.: Investigations of emissions and heterogeneous formation of HONO in a road traffic tunnel, Atmos. Environ., 35, 3385-3394, 10.1016/s1352-2310(01)00138-8, 2001.

Li, J., Wang, Z., Wang, X., Yamaji, K., Takigawa, M., Kanaya, Y., Pochanart, P., Liu, Y., Irie, H., Hu, B., Tanimoto, H., and Akimoto, H.: Impacts of aerosols on summertime tropospheric photolysis frequencies and photochemistry over Central Eastern China, Atmos. Environ., 45, 1817-1829, https://doi.org/10.1016/j.atmosenv.2011.01.016, 2011.

Li, J., Chen, X. S., Wang, Z. F., Du, H. Y., Yang, W. Y., Sun, Y. L., Hu, B., Li, J. J., Wang, W., Wang, T., Fu, P. Q., and Huang, H. L.: Radiative and heterogeneous chemical effects of aerosols on ozone and inorganic aerosols over East Asia, Sci. Total Environ., 622, 1327-1342, 10.1016/j.scitotenv.2017.12.041, 2018a.

Li, K., Jacob, D. J., Liao, H., Shen, L., Zhang, Q., and Bates, K. H.: Anthropogenic drivers of 2013-2017 trends in summer surface ozone in China, P Natl Acad Sci USA, 116, 422-427, 2019.

Li, S. W., Liu, W. Q., Xie, P. H., Qin, M., and Yang, Y. J.: Observation of Nitrate Radical in the Nocturnal Boundary Layer During a Summer Field Campaign in Pearl River Delta, China, Terr Atmos Ocean Sci, 23, 39-48, 10.3319/Tao.2011.07.26.01(a), 2012a.

Li, X., Brauers, T., Häseler, R., Bohn, B., Fuchs, H., Hofzumahaus, A., Holland, F., Lou, S., Lu, K. D., Rohrer, F., Hu, M., Zeng, L. M., Zhang, Y. H., Garland, R. M., Su, H., Nowak, A., Wiedensohler, A., Takegawa, N., Shao, M., and Wahner, A.: Exploring the atmospheric chemistry of nitrous acid (HONO) at a rural site in Southern China, Atmos. Chem. Phys., 12, 1497-1513, 10.5194/acp-12-1497-2012, 2012b.

Li, Z. Y., Xue, L. K., Yang, X., Zha, Q. Z., Tham, Y. J., Yan, C., Louie, P. K. K., Luk, C. W. Y., Wang, T., and Wang, W. X.: Oxidizing capacity of the rural atmosphere in Hong Kong, Southern China, Sci. Total Environ., 612, 1114-1122, 10.1016/j.scitotenv.2017.08.310, 2018b.

Liang, H., Chen, Z. M., Huang, D., Zhao, Y., and Li, Z. Y.: Impacts of aerosols on the chemistry of atmospheric trace gases: a case study of peroxides and HO₂ radicals, Atmos. Chem. Phys., 13, 11259-11276, 10.5194/acp-13-11259-2013, 2013.

Liao, H., Seinfeld, J. H., Adams, P. J., and Mickley, L. J.: Global radiative forcing of coupled tropospheric ozone and aerosols in a unified general circulation model, J Geophys Res-Atmos, 109, 2004.

Liao, H., and Seinfeld, J. H.: Global impacts of gas-phase chemistry-aerosol interactions on direct radiative forcing by anthropogenic aerosols and ozone, J Geophys Res-Atmos, 110, 22, 10.1029/2005jd005907, 2005.

Liu, Y., and Wang, T.: Worsening urban ozone pollution in China from 2013 to 2017 – Part 1: The complex and varying roles of meteorology, Atmos. Chem. Phys. Discuss., 2020, 1-28, 10.5194/acp-2019-1120, 2020.

Longfellow, C. A., Ravishankara, A. R., and Hanson, D. R.: Reactive and nonreactive uptake on hydrocarbon soot: HNO3, O3, and N2O5, 105, 24345-24350, 10.1029/2000jd900297, 2000.

Lou, S. J., Liao, H., and Zhu, B.: Impacts of aerosols on surface-layer ozone concentrations in China through heterogeneous reactions and changes in photolysis rates, Atmos. Environ., 85, 123-138, 10.1016/j.atmosenv.2013.12.004, 2014.

Lu, K. D., Rohrer, F., Holland, F., Fuchs, H., Bohn, B., Brauers, T., Chang, C. C., Häseler, R., Hu, M., Kita, K., Kondo, Y., Li, X., Lou, S. R., Nehr, S., Shao, M., Zeng, L. M., Wahner, A., Zhang, Y. H., and Hofzumahaus, A.: Observation and modelling of OH and HO₂ concentrations in the Pearl River Delta 2006: a missing OH source in a VOC rich atmosphere, Atmos. Chem. Phys., 12, 1541-1569, 10.5194/acp-12-1541-2012, 2012.

Lu, K. D., Hofzumahaus, A., Holland, F., Bohn, B., Brauers, T., Fuchs, H., Hu, M., Häseler, R., Kita, K., Kondo, Y., Li, X., Lou, S. R., Oebel, A., Shao, M., Zeng, L. M., Wahner, A., Zhu, T., Zhang, Y. H., and Rohrer, F.: Missing OH source in a suburban environment near Beijing: observed and modelled OH and HO₂ concentrations in summer 2006, Atmos. Chem. Phys., 13, 1057-1080, 10.5194/acp-13-1057-2013, 2013.

Lu, X., Hong, J. Y., Zhang, L., Cooper, O. R., Schultz, M. G., Xu, X. B., Wang, T., Gao, M., Zhao, Y. H., and Zhang, Y. H.:

Severe Surface Ozone Pollution in China: A Global Perspective, Environ Sci Tech Let, 5, 487-494, 10.1021/acs.estlett.8b00366, 2018.

Mao, J. Q., Paulot, F., Jacob, D. J., Cohen, R. C., Crounse, J. D., Wennberg, P. O., Keller, C. A., Hudman, R. C., Barkley, M. P., and Horowitz, L. W.: Ozone and organic nitrates over the eastern United States: Sensitivity to isoprene chemistry, J Geophys Res-Atmos, 118, 11256-11268, 2013.

Michel, A. E., Usher, C. R., and Grassian, V. H.: Heterogeneous and catalytic uptake of ozone on mineral oxides and dusts: A Knudsen cell investigation, 29, 10-11-10-14, 10.1029/2002gl014896, 2002.

Michel, A. E., Usher, C. R., and Grassian, V. H.: Reactive uptake of ozone on mineral oxides and mineral dusts, Atmos. Environ., 37, 3201-3211, https://doi.org/10.1016/S1352-2310(03)00319-4, 2003.

Moise, T., Talukdar, R. K., Frost, G. J., Fox, R. W., and Rudich, Y.: Reactive uptake of NO3 by liquid and frozen organics, 107, AAC 6-1-AAC 6-9, 10.1029/2001jd000334, 2002.

Ndour, M., D'Anna, B., George, C., Ka, O., Balkanski, Y., Kleffmann, J., Stemmler, K., and Ammann, M.: Photoenhanced uptake of NO2 on mineral dust: Laboratory experiments and model simulations, 35, 10.1029/2007gl032006, 2008.

NRC: Rethinking the Ozone Problem in Urban and Regional Air Pollution, National Academy Press, Washington, DC, 1991.

Pozzoli, L., Bey, I., Rast, S., Schultz, M. G., Stier, P., and Feichter, J.: Trace gas and aerosol interactions in the fully coupled model of aerosol-chemistry-climate ECHAM5-HAMMOZ: 1. Model description and insights from the spring 2001 TRACE-P experiment, 113, 10.1029/2007jd009007, 2008.

Qin, M., Xie, P., Su, H., Gu, J., Peng, F., Li, S., Zeng, L., Liu, J., Liu, W., and Zhang, Y.: An observational study of the HONO–NO2 coupling at an urban site in Guangzhou City, South China, Atmos. Environ., 43, 5731-5742, https://doi.org/10.1016/j.atmosenv.2009.08.017, 2009.

Qin, M. R., Chen, Z. M., Shen, H. Q., Li, H., Wu, H. H., and Wang, Y.: Impacts of heterogeneous reactions to atmospheric peroxides: Observations and budget analysis study, Atmos. Environ., 183, 144-153, 10.1016/j.atmosenv.2018.04.005, 2018.

Ramanathan, V., and Carmichael, G.: Global and regional climate changes due to black carbon, Nat Geosci, 1, 221-227, 10.1038/ngeo156, 2008.

Rudich, Y., Talukdar, R. K., Ravishankara, A. R., and Fox, R. W.: Reactive uptake of NO3 on pure water and ionic solutions, 101, 21023-21031, 10.1029/96jd01844, 1996.

Sarwar, G., Simon, H., Bhave, P., and Yarwood, G.: Examining the impact of heterogeneous nitryl chloride production on air quality across the United States, Atmos Chem Phys, 12, 6455-6473, 10.5194/acp-12-6455-2012, 2012.

Stadtler, S., Simpson, D., Schröder, S., Taraborrelli, D., Bott, A., and Schultz, M.: Ozone impacts of gas–aerosol uptake in global chemistry transport models, Atmos. Chem. Phys., 18, 3147-3171, 10.5194/acp-18-3147-2018, 2018.

Stemmler, K., Ndour, M., Elshorbany, Y., Kleffmann, J., D'Anna, B., George, C., Bohn, B., and Ammann, M.: Light induced conversion of nitrogen dioxide into nitrous acid on submicron humic acid aerosol, Atmos. Chem. Phys., 7, 4237-4248, 10.5194/acp-7-4237-2007, 2007.

Stutz, J., Alicke, B., Ackermann, R., Geyer, A., Wang, S., White, A. B., Williams, E. J., Spicer, C. W., and Fast, J. D.: Relative humidity dependence of HONO chemistry in urban areas, 109, 10.1029/2003jd004135, 2004.

Tan, Z., Fuchs, H., Lu, K., Hofzumahaus, A., Bohn, B., Broch, S., Dong, H., Gomm, S., Häseler, R., He, L., Holland, F., Li, X., Liu, Y., Lu, S., Rohrer, F., Shao, M., Wang, B., Wang, M., Wu, Y., Zeng, L., Zhang, Y., Wahner, A., and Zhang, Y.: Radical chemistry at a rural site (Wangdu) in the North China Plain: observation and model calculations of OH, HO2 and RO2 radicals, Atmos. Chem. Phys., 17, 663-690, 10.5194/acp-17-663-2017, 2017.

Tham, Y. J., Yan, C., Xue, L. K., Zha, Q. Z., Wang, X. F., and Wang, T.: Presence of high nitryl chloride in Asian coastal environment and its impact on atmospheric photochemistry, Chinese Sci Bull, 59, 356-359, 10.1007/s11434-013-0063-y, 2014.

Tham, Y. J., Wang, Z., Li, Q., Yun, H., Wang, W., Wang, X., Xue, L., Lu, K., Ma, N., Bohn, B., Li, X., Kecorius, S., Größ, J., Shao, M., Wiedensohler, A., Zhang, Y., and Wang, T.: Significant concentrations of nitryl chloride sustained in the morning: investigations of the causes and impacts on ozone production in a polluted region of northern China, Atmos. Chem. Phys., 16, 14959-14977, 10.5194/acp-16-14959-2016, 2016.

Wang, J. Q., Zhang, X. S., Guo, J., Wang, Z. W., and Zhang, M. G.: Observation of nitrous acid (HONO) in Beijing, China: Seasonal variation, nocturnal formation and daytime budget, Sci. Total Environ., 587, 350-359, 10.1016/j.scitotenv.2017.02.159, 2017a.

Wang, N., Lyu, X. P., Deng, X. J., Huang, X., Jiang, F., and Ding, A. J.: Aggravating O-3 pollution due to NOx emission control in eastern China, Sci. Total Environ., 677, 732-744, 10.1016/j.scitotenv.2019.04.388, 2019a.

Wang, P. F., Guo, H., Hu, J. L., Kota, S. H., Ying, Q., and Zhang, H.: Responses of PM2.5 and O-3 concentrations to changes of meteorology and emissions in China, Sci. Total Environ., 662, 297-306, 10.1016/j.scitotenv.2019.01.227, 2019b.

Wang, S. S., Shi, C. Z., Zhou, B., Zhao, H., Wang, Z. R., Yang, S. N., and Chen, L. M.: Observation of NO3 radicals over Shanghai, China, Atmos. Environ., 70, 401-409, 10.1016/j.atmosenv.2013.01.022, 2013.

Wang, T., Xue, L. K., Brimblecombe, P., Lam, Y. F., Li, L., and Zhang, L.: Ozone pollution in China: A review of concentrations, meteorological influences, chemical precursors, and effects, Sci. Total Environ., 575, 1582-1596, 10.1016/j.scitotenv.2016.10.081, 2017b.

Wang, T., Dai, J., Lam, K. S., Nan Poon, C., and Brasseur, G. P.: Twenty-Five Years of Lower Tropospheric Ozone Observations in Tropical East Asia: The Influence of Emissions and Weather Patterns, 46, 11463-11470, 10.1029/2019gl084459, 2019c.

Wang, Y., Chen, Z., Wu, Q., Liang, H., Huang, L., Li, H., Lu, K., Wu, Y., Dong, H., Zeng, L., and Zhang, Y.: Observation of atmospheric peroxides during Wangdu Campaign 2014 at a rural site in the North China Plain, Atmos. Chem. Phys., 16, 10985-11000, 10.5194/acp-16-10985-2016, 2016.

Wang, Z., Wang, W., Tham, Y. J., Li, Q., Wang, H., Wen, L., Wang, X., and Wang, T.: Fast heterogeneous N2O5 uptake and ClNO2 production in power plant and industrial plumes observed in the nocturnal residual layer over the North China Plain, Atmos. Chem. Phys., 17, 12361-12378, 10.5194/acp-17-12361-2017, 2017c.

Xing, J., Wang, S. X., Jang, C., Zhu, Y., and Hao, J. M.: Nonlinear response of ozone to precursor emission changes in China: a modeling study using response surface methodology, Atmos. Chem. Phys., 11, 5027-5044, 10.5194/acp-11-5027-2011, 2011.

Xing, J., Wang, J., Mathur, R., Wang, S., Sarwar, G., Pleim, J., Hogrefe, C., Zhang, Y., Jiang, J., Wong, D. C., and Hao, J.: Impacts of aerosol direct effects on tropospheric ozone through changes in atmospheric dynamics and photolysis rates, Atmos. Chem. Phys., 17, 9869-9883, 10.5194/acp-17-9869-2017, 2017.

Xu, X., Lin, W., Xu, W., Jin, J., Wang, Y., Zhang, G., Zhang, X., Ma, Z., Dong, Y., Ma, Q., Yu, D., Li, Z., Wang, D., and Zhao, H.: Long-term changes of regional ozone in China: implications for human health and ecosystem impacts, Elem Sci Anth, 8, 13, 10.1525/elementa.409, 2020.

Xu, Z., Wang, T., Wu, J. Q., Xue, L. K., Chan, J., Zha, Q. Z., Zhou, S. Z., Louie, P. K. K., and Luk, C. W. Y.: Nitrous acid (HONO) in a polluted subtropical atmosphere: Seasonal variability, direct vehicle emissions and heterogeneous production at ground surface, Atmos. Environ., 106, 100-109, 10.1016/j.atmosenv.2015.01.061, 2015.

Yan, C., Tham, Y. J., Zha, Q. Z., Wang, X. F., Xue, L. K., Dai, J. N., Wang, Z., and Wang, T.: Fast heterogeneous loss of N2O5 leads to significant nighttime NOx removal and nitrate aerosol formation at a coastal background environment of southern China, Sci. Total Environ., 677, 637-647, 10.1016/j.scitotenv.2019.04.389, 2019.

Yu, Y., Wang, Z., He, T., Meng, X., Xie, S., and Yu, H.: Driving factors of the significant increase in surface ozone in the Yangtze River Delta, China, during 2013–2017, Atmospheric Pollution Research, 10, 1357-1364, 10.1016/j.apr.2019.03.010, 2019.

Zhang, Q., Zheng, Y. X., Tong, D., Shao, M., Wang, S. X., Zhang, Y. H., Xu, X. D., Wang, J. N., He, H., Liu, W. Q., Ding, Y. H., Lei, Y., Li, J. H., Wang, Z. F., Zhang, X. Y., Wang, Y. S., Cheng, J., Liu, Y., Shi, Q. R., Yan, L., Geng, G. N., Hong, C. P., Li, M., Liu, F., Zheng, B., Cao, J. J., Ding, A. J., Gao, J., Fu, Q. Y., Huo, J. T., Liu, B. X., Liu, Z. R., Yang, F. M., He, K. B., and Hao, J. M.: Drivers of improved PM2.5 air quality in China from 2013 to 2017, P Natl Acad Sci USA, 116, 24463-24469, 10.1073/pnas.1907956116, 2019.

Zhang, Y., and Carmichael, G. R.: The role of mineral aerosol in tropospheric chemistry in East Asia - A model study, J Appl Meteorol, 38, 353-366, 1999.

Zheng, B., Tong, D., Li, M., Liu, F., Hong, C., Geng, G., Li, H., Li, X., Peng, L., Qi, J., Yan, L., Zhang, Y., Zhao, H., Zheng, Y., He, K., and Zhang, Q.: Trends in China's anthropogenic emissions since 2010 as the consequence of clean air actions, Atmos. Chem. Phys., 18, 14095-14111, 10.5194/acp-18-14095-2018, 2018.

Zhu, S., Butler, T., Sander, R., Ma, J., and Lawrence, M. G.: Impact of dust on tropospheric chemistry over polluted regions: a case study of the Beijing megacity, Atmos Chem Phys, 10, 3855-3873, 10.5194/acp-10-3855-2010, 2010.

Figure 1: Trends of simulated MDA8 O_3 mixing ratios averaged in urban and rural areas and all land areas of China in summer (June-August) from 2013 to 2017. See Fig. S3 for the locations of urban and rural areas over China.

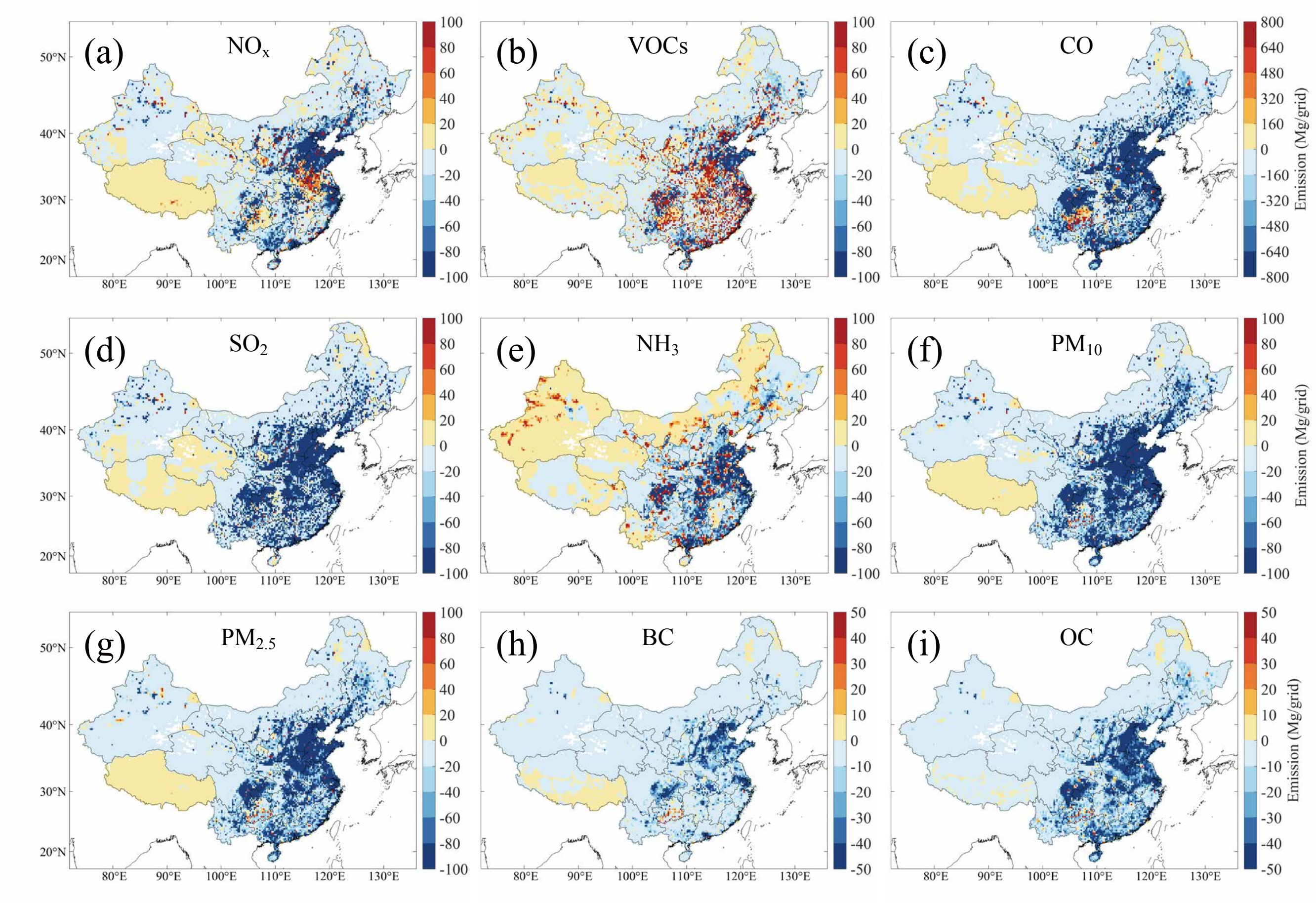

Figure 2: Spatial distributions of changes in anthropogenic pollutant emissions in the summer of 2017 relative to that of 2013, including (a) NO_x, (b) VOCs, (c) CO, (d) SO_2, (e) NH_3, (f) PM_{10}, (g) $PM_{2.5}$, (h) BC, and (i) OC. Emission data are obtained from Multi-resolution Emission Inventory for China (MEIC; http://www.meicmodel.org).

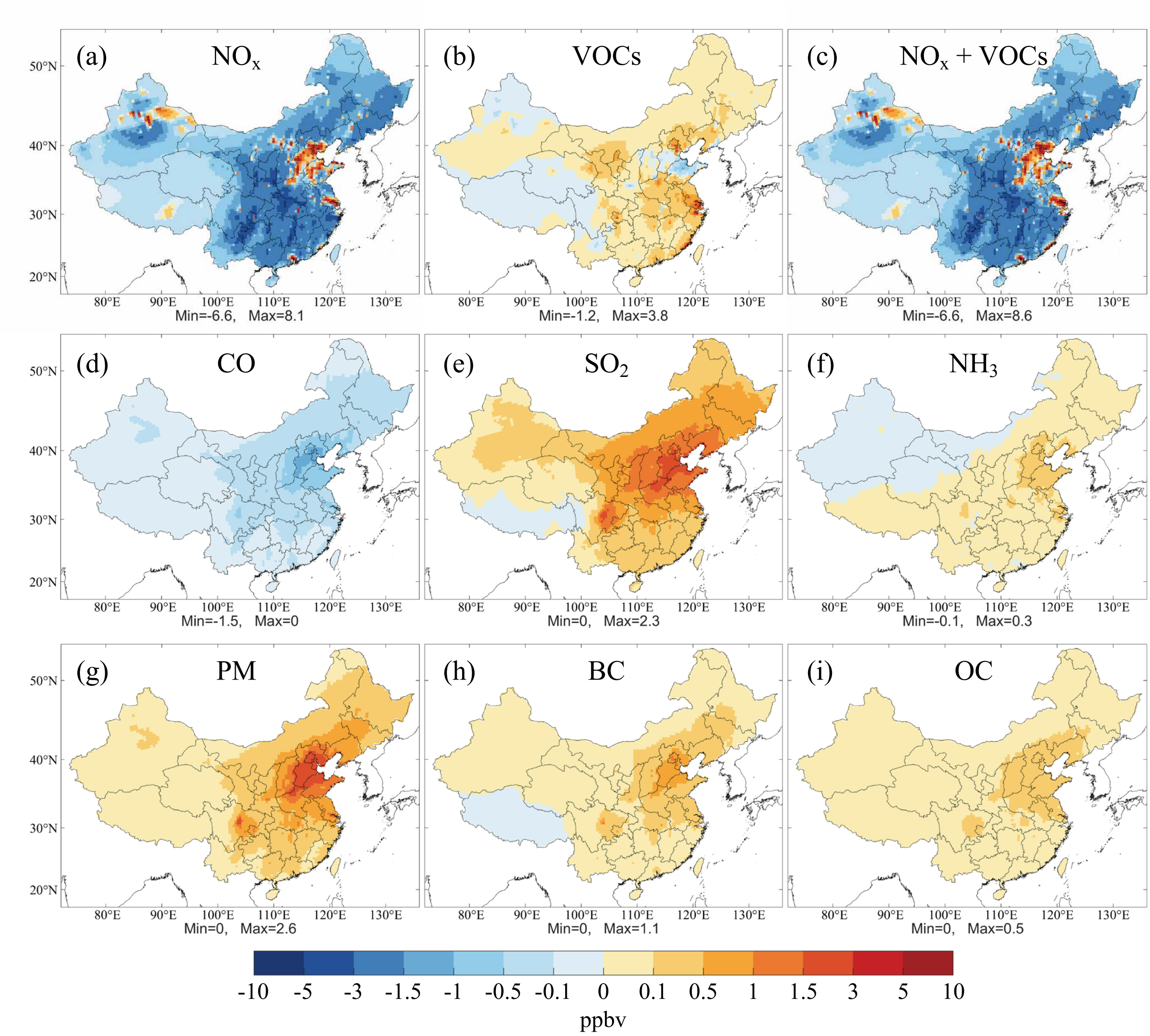

605 **Figure 3: Spatial distribution of the simulated MDA8 O_3 mixing ratios responding to the changes of individual pollutant emissions in summer from 2013 to 2017, including (a) NO_x, (b) VOCs, (c) NO_x and VOCs, (d) CO, (e) SO_2, (f) NH_3, (g) PM, (h) BC, and (i) OC.**

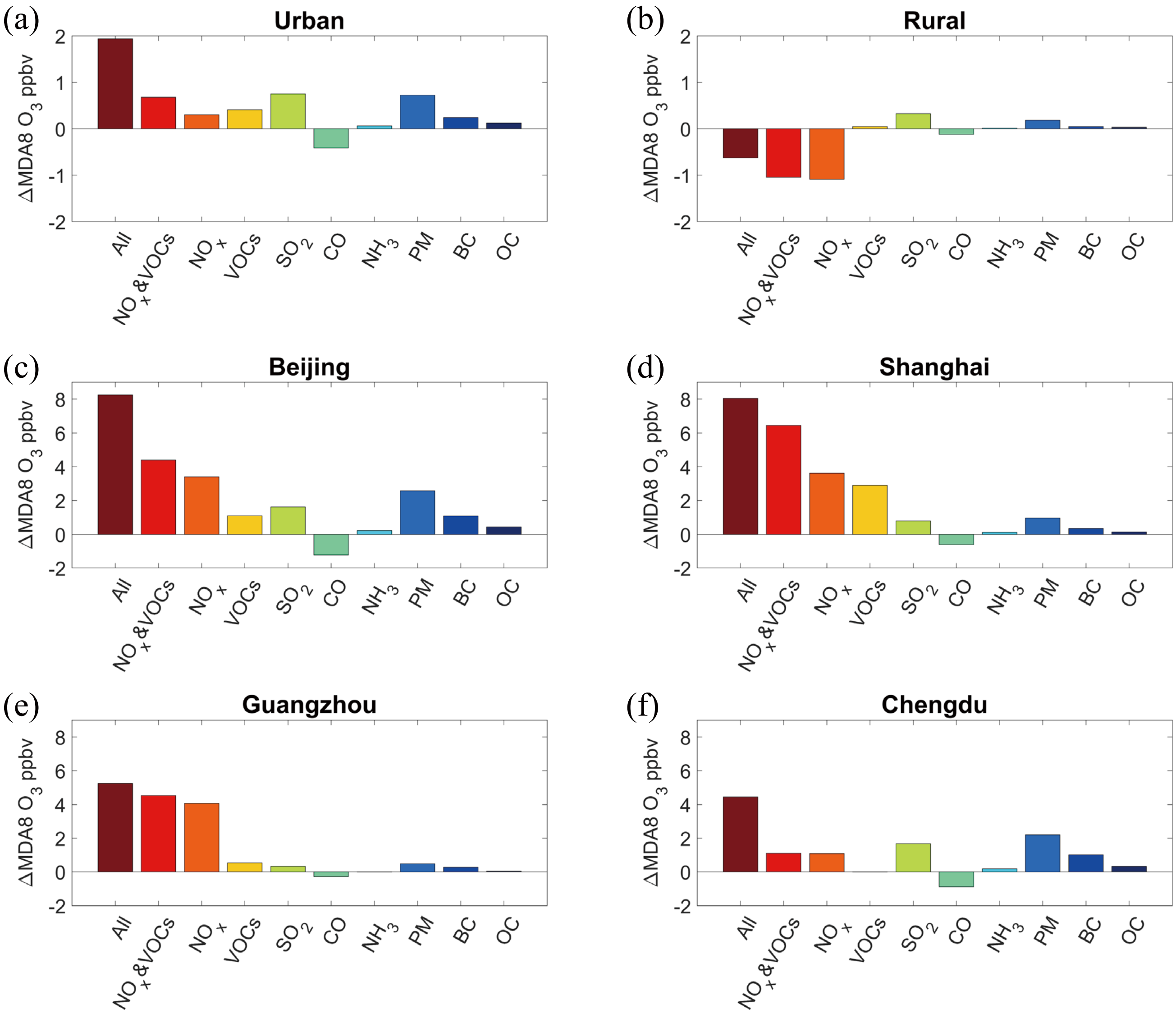

Figure 4: Response of the simulated MDA8 O_3 mixing ratios to the changes in individual pollutant emissions in summer from 2013 to 2017 in (a) the urban areas, (b) the rural areas, (c) Beijing, (d) Shanghai, (e) Guangzhou, and (f) Chengdu. See Fig. S1 in part 1 (Liu and Wang, 2020) for the locations of the four megacities.

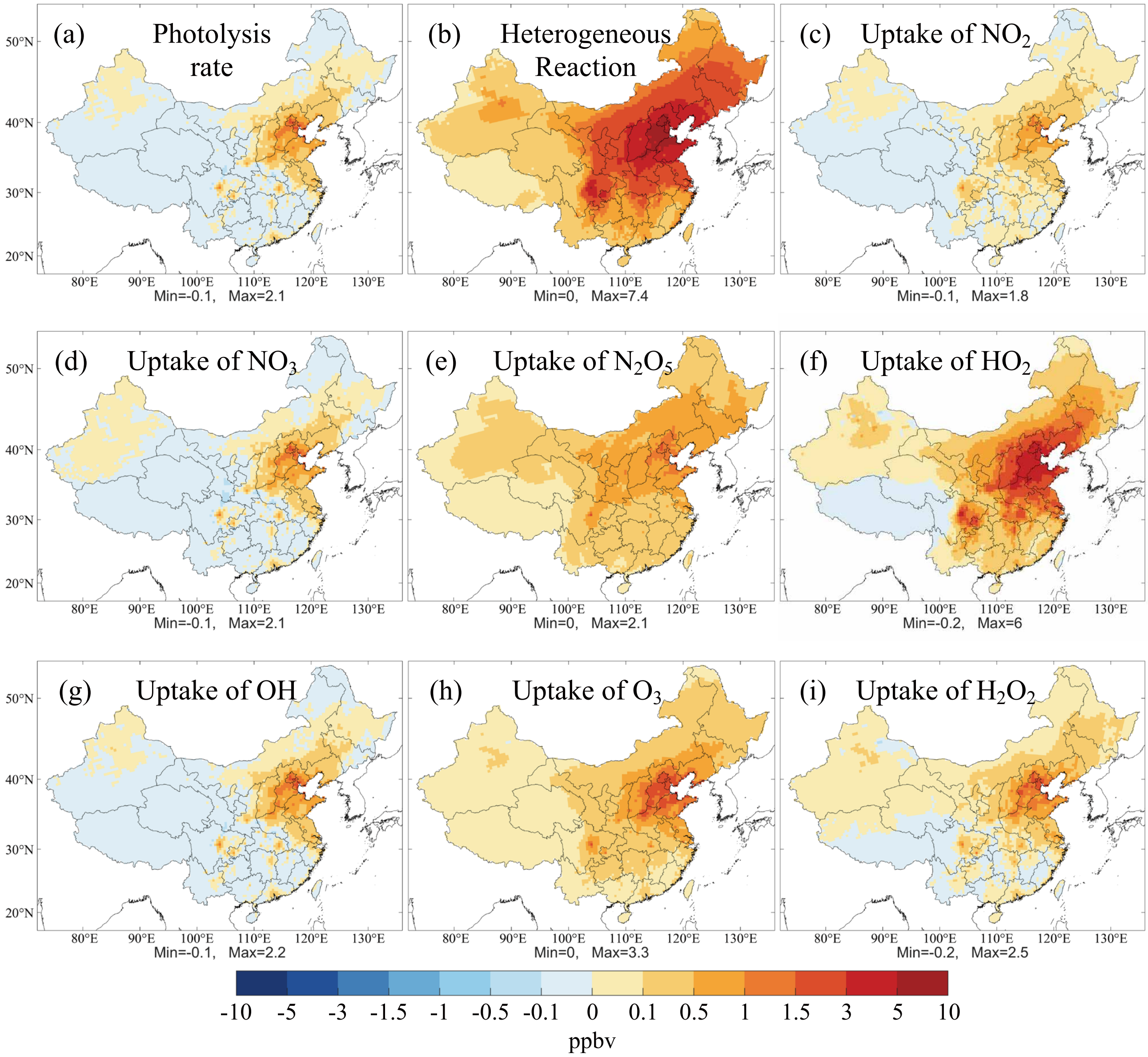

Figure 5: Spatial distribution of the simulated MDA8 O_3 mixing ratios responding to the changes in the effects of aerosol in summer 615 **from 2013 to 2017 (see Methods). The aerosol affects O_3 via altering (a) photolysis rates, (b) all heterogeneous reactions, and individual heterogeneous reactions, namely the uptake of (c) NO_2, (d) NO_3, (e) N_2O_5, (f) HO_2, (g) OH, (h) O_3, and (i) H_2O_2.**

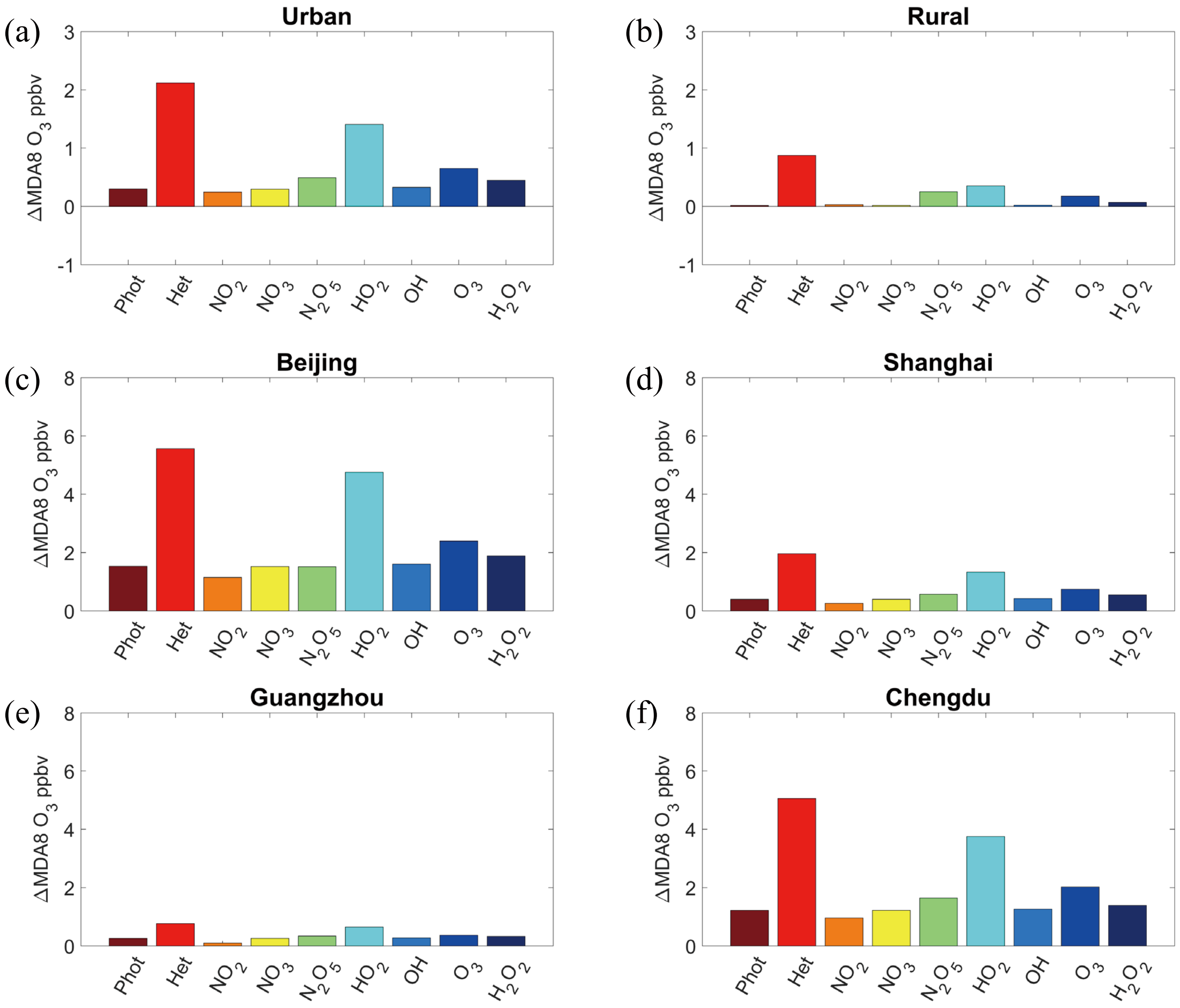

Figure 6: Response of the simulated MDA8 O_3 mixing ratios to the changes in the effects of aerosols in summer from 2013 to 2017 in (a) the urban area, (b) the rural area, (c) Beijing, (d) Shanghai, (e) Guangzhou, and (f) Chengdu. The aerosol affects O_3 via altering the photolysis rates (Phot), all heterogeneous reactions (Het), and individual heterogeneous reactions, namely the uptake of NO_2, NO_3, N_2O_5, HO_2, OH, O_3, and H_2O_2.

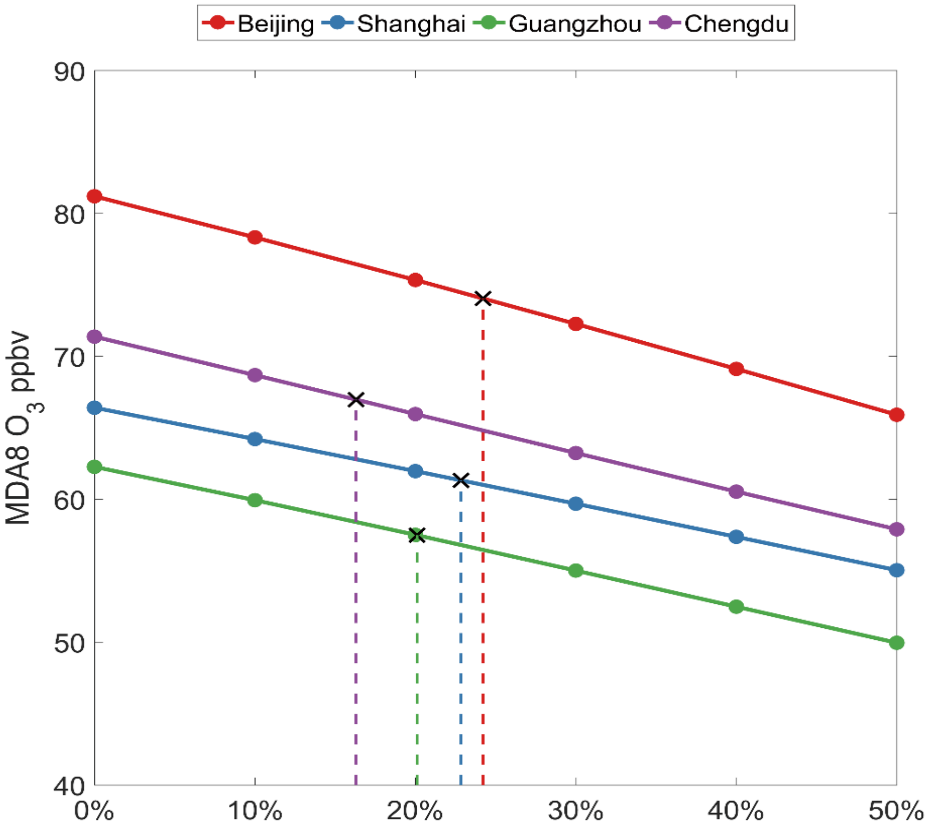

625 **Figure 7: Response of simulated MDA8 O_3 mixing ratios with 2017 emissions (except for VOCs) to the reductions of anthropogenic VOCs from the 2013 level in summer in Beijing, Shanghai, Guangzhou, and Chengdu. The black crosses depict the MDA8 values in 2013 and the required reduction of VOCs emissions in 2017 to maintain the 2013 O_3 level in each city.**